Separation-Based Adsorption of H_2 from Binary Mixtures inside Single, Double, Triple Walled Boron-Nitride Nanotubes: A Grand-Canonical Monte-Carlo Study

Zohreh Ahadi[a], Muhammad Shadman Lakmehsari[b], Vahid Sokhanvaran[c], Jamal Davoodi[a,*]

[a] Department of Physics, Faculty of Science, University of Zanjan, P.O. Box 45195-313, Zanjan, Iran.

[b] Department of Chemistry, Faculty of Science, University of Zanjan, P.O. Box 45195-313, Zanjan, Iran.

[c] Department of Chemistry, Faculty of Basic Sciences, University of Neyshabur, Neyshabur, Iran.

*corresponding author: jdavoodi@znu.ac.ir (J Davoodi)

Graphical abstract:

B (pink), N (blue), H_2 (red) and He (gray) are represented. The single, double and triple walled are (29,29), (7,7)@(22,22) and (7,7)@(15,15)@(22,22) respectively.
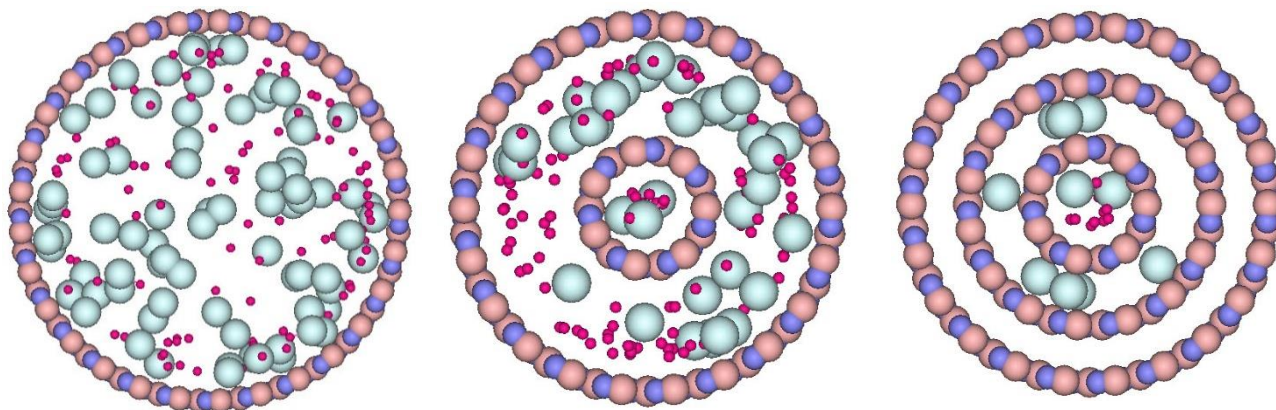
Abstract

This study investigates the separation based on adsorption of the binary gas mixture of hydrogen with biogas (gases: CO_2, CH_4, O_2, N_2) and inert gases (gases: He, Ne, and Ar) using single-walled ((7,7), (15,15), (29,29), (44,44), (58,58) and (73,73) SWBNNTs), double-walled ((11,11)@(15,15), (7,7)@(22,22) DWBNNTs) and triple walled ((8,8)@(11,11)@(15,15) and (7,7)@(15,15)@(22,22) TWBNNTs) boron nitride nanotubes via the grand canonical Monte Carlo (GCMC) simulation. Two models, namely, spherical and site-site models, are employed for gas. Two conditions are used for the SWBNNTs, i.e., SWBNNTs with atomic charges and SWBNNTs without atomic charges. This paper also examines the impact of nanotube diameters on binary mixture adsorption. The results indicate that considering the H_2/gas separation in the studied BNNTs, the H_2 separation from He and the H_2 separation from Ar have the maximum and minimum selectivity values, respectively. Also, with increasing pressure and temperature, the values of the H_2/He selectivity in the studied BNNTs decrease.

1. Introduction

Boron nitride nanotubes (BNNTs) were theoretically predicted by Rubio in 1994 [1, 2], and then, they were experimentally synthesized by Chopra et al. [1, 3]. Recently, BNNTs have attracted numerous attention due to their outstanding characteristics. These characteristics are unique to BNNTs and are not found in other nanomaterials. The structure of BNNTs is similar to that of carbon nanotubes (CNTs); however, the properties of BNNTs are noticeably different from those of CNTs [4]. In addition, unlike CNTs, BNNTs possess special physicochemical properties, which enables them to have potential applications in nanotechnologies. [5]. Therefore, BNNTs show incredible guarantee in various potential fields, for example, optical frameworks, electrical

nanodevices, energy storage, atomic reactor offices, radiation protecting in space vehicles [6], Hydrogen storage and sensing application [7], and biomedical and medical and applications [4]. Also, BNNTs are considered as a valuable platform for constructing new materials which are useful for various applications [8]. They have unique properties, such as high chemical stability, excellent mechanical properties, and high thermal conductivity [9]. Also, BNNTs possess approximately uniform electronic properties, tunable band gaps (~5 eV), and high oxidation resistance. In addition, BNNTs have piezoelectric properties, which makes them useful for room-temperature hydrogen storage [10]. The difference between the properties of BNNTs and CNTs is as follows: the electronic structure of pure CNTs is either metallic or semiconducting; therefore, CNTs are sensitive to tube diameters, wrapping angles, and twisting and topological defects while a wide band gap of BNNTs is sensitive neither to tube diameters nor to chiral angels. The gaps of BNNTs can be controlled by chemical composition because of the ionic origin of their band gaps. Strong ionic bonds between Boron atoms and nitrogen atoms also have considerable effects on the formation of BNNTs [11]. The physisorption properties of a Boron Nanotube are enhanced because of the dipolar fields close to its surface. The high specific surface area (SSA) of Boron Nitrides (BNs) makes it possible to store gases, such as hydrogen, and makes BNs much more effective than CNTs [12]. Gas separation, such as H_2 separation, is essential to come up with new clean energy techniques. A lot of materials have been developed for the purpose of investigating gas separation [13]. To obtain the highly efficient separation of gas mixtures via adsorption, the selection of proper adsorbents is of critical importance [14]. Mpourmpakis and Froudakis indicated that BNNTs were more sutiable materials for H_2 storage than CNTs because the BNNTs bonds had the ionic properties and these properties could enhance the binding energy of hydrogen. [15]. Hydrogen is considered as the most encouraging

energy carrier and holds colossal guarantee as a clean and renewable energy alternative. Hydrogen is a helpful, safe, and flexible fuel source which can undoubtedly be converted into an ideal type of energy without discharging destructive emissions. Hydrogen is a perfect fuel since it significantly reduces greenhouse gas emissions, decreases global dependence on fossil fuels, and increases the efficiency of energy conversion [16]. Hydrogen adsorption on porous materials is one of the possible methods of hydrogen separation. The most common adsorbents used for H_2 separation are activated carbon [17], zeolites [18, 19] silica-based adsorbents [20], carbon nanotubes [21, 22] and metal-organic frameworks [23, 24]. Thus, a variety of porous materials have been investigated, particularly through molecular simulation methods, and their selective adsorption behaviors and separation capacities have been detected. To achieve the optimal separation capacities, perfect microporous materials should augment the adsorption limits of their hydrogen and decrease the adsorption capacities of other species [25]. Among the diverse technologies propounded for such separation purposes, physisorption using porous materials is a very promising cost-efficient technology. BNNTs are one of the main groups of materials that have been widely used as promising materials for hydrogen separation. To the best of the researcher's knowledge, there are just a few computational and experimental studies focusing on the separation of H_2 from two groups of gases (biogas and noble gases) using BNNTs. Therefore, this study aimed to examine H_2 separation from biogas and noble gases using single-walled and multi-walled BNNTs via the GCMC simulations.

In the next section, the methods used in this study, including the details of the developed force fields and the way the Monte Carlo method is employed, are explained. The results of the simulations are reported in the subsequent sections.

2. Computational method

In this paper, to investigate the role of BNNTs in the separation of hydrogen from H_2/gas (gases: CO_2, CH_4, O_2, N_2, He, Ne, and Ar), the Monte Carlo molecular simulation is performed in the grand canonical ensemble. The (7,7), (15,15), (29,29), (44,44), (58,58) and (73,73) single-walled BNNTs (SWBNNTs), (11,11)@(15,15) and (7,7)@(22,22) double-walled BNNTs (DWBNNTs), and (8,8)@(11,11)@(15,15) and (7,7)@(15,15)@(22,22) triple-walled BNNTs (TWBNNTs) are used. The structure of the nanotubes is kept rigid. Moreover, the geometry variation of the adsorbents is overlooked since the geometric variation of nanotubes caused by gases can be neglected at room temperature. The logic behind the GCMC simulations is provided in the literature [26-29]. The multipurpose simulation code (the MUSIC code) of the molecular simulation package is used for all the GCMC simulations [30]. In all simulations, 4×10^7 of iterations were considered. The first half of iterations are used to set up the equilibrium of the system and the last half of iteration is used to calculate the ensemble average values of the thermodynamic parameters. The separation of hydrogen from gases depends on its selectivity. The hydrogen selectivity refers to the ratio of the mole fraction of hydrogen in the pore and bulk phases over the ratio of the mole fraction of the gas in the binary mixture in the pore and bulk phases [29].

The periodic boundary condition (PBC) is applied in the tube length direction while the cutoff distance is set a bit smaller than half the size of the simulation cell. It shoulde be noted the largest and the smallest boxes have $100.4 \times 100.4 \times 39.9$ Å^3 and $10.7 \times 10.7 \times 42.1$ Å^3 respectivley. In this paper, all the gases are treated using two models: the one-site (spherical) model and the site-site model. The spherical model is the simplest 12-6 Lennard–Jones (LJ) potential for calculating the molecule interactions with each other and with the B and N atoms of BNNTs. The LJ parameters for different atoms are calculated by the Lorentz–Berthelot (LB) mixing rules.

The 12-6 LJ potential parameters of spherical gas molecules and BNNT atoms are reported in [26, 27, 31]. Regarding the site-site model, the nanotube atoms are examined with and without atomic charges. The 12-6 LJ potential parameters of the gas site-site model are presented in [32] and the atomic charges of BNNTs are reported in [33]. The Wolf method is used for modeling electrostatic interactions.

3. Results and discussion

The GCMC simulations are carried out to delve into the separation-based adsorption of H_2/gas (i.e., the binary mixtures including H_2). The following sections present the H2/gas selectivity in the SWBNNTs, DWBNNTs, and TWBNNTs, respectively. It sould be noted that all gas adsorption on the studied BNNTs is based on physisorption and the maximum energy of adsorption was obtained about 5 ± 0.3 $kJmol^{-1}$.

3.1. H_2/gas selectivity in SWBNNTs

At first, the adsorption selectivity of the binary mixtures of H_2/gas (gases: Ar, CH_4, CO_2, He, N_2, Ne, and O_2) is simulated inside the single-walled BNNTs (SWBNNTs). The values are displayed in Figure 1. As shown in Figure 1, the maximum values of the H_2/gas selectivity in the (7,7) SWBNNT, in the (15,15) SWBNNT, and in the (29,29) SWBNNT are $S_{H2/He}=3.31$ at P=2.5 MPa, $S_{H2/He}=3.5$ at P=2.5 MPa, and $S_{H2/He}=3.86$ at 10 MPa, respectively. The values of the H_2/He selectivity in these SWBNNTs decrease as pressure increases. In the (7,7) SWBNNT, the H_2/CO_2 selectivity initially increases followed by a plateau phase at 8 MPa. In the (15,15) SWBNNT, the H_2/O_2 selectivity fluctuates in the form of zigzag curves. The order of the selectivity values of other gases is as follows: in the (7,7) SWBNN: H_2/CH_4> H_2/N_2> H_2/O_2> H_2/Ar> H_2/Ne; in the (15,15) SWBNN: H_2/Ne> H_2/Ar> H_2/CO_2> H_2/CH4> H_2/N_2; and in the (29,29) SWBNN: H_2/ Ne > H_2/CO_2> H_2/N_2> H_2/He> H_2/Ar.
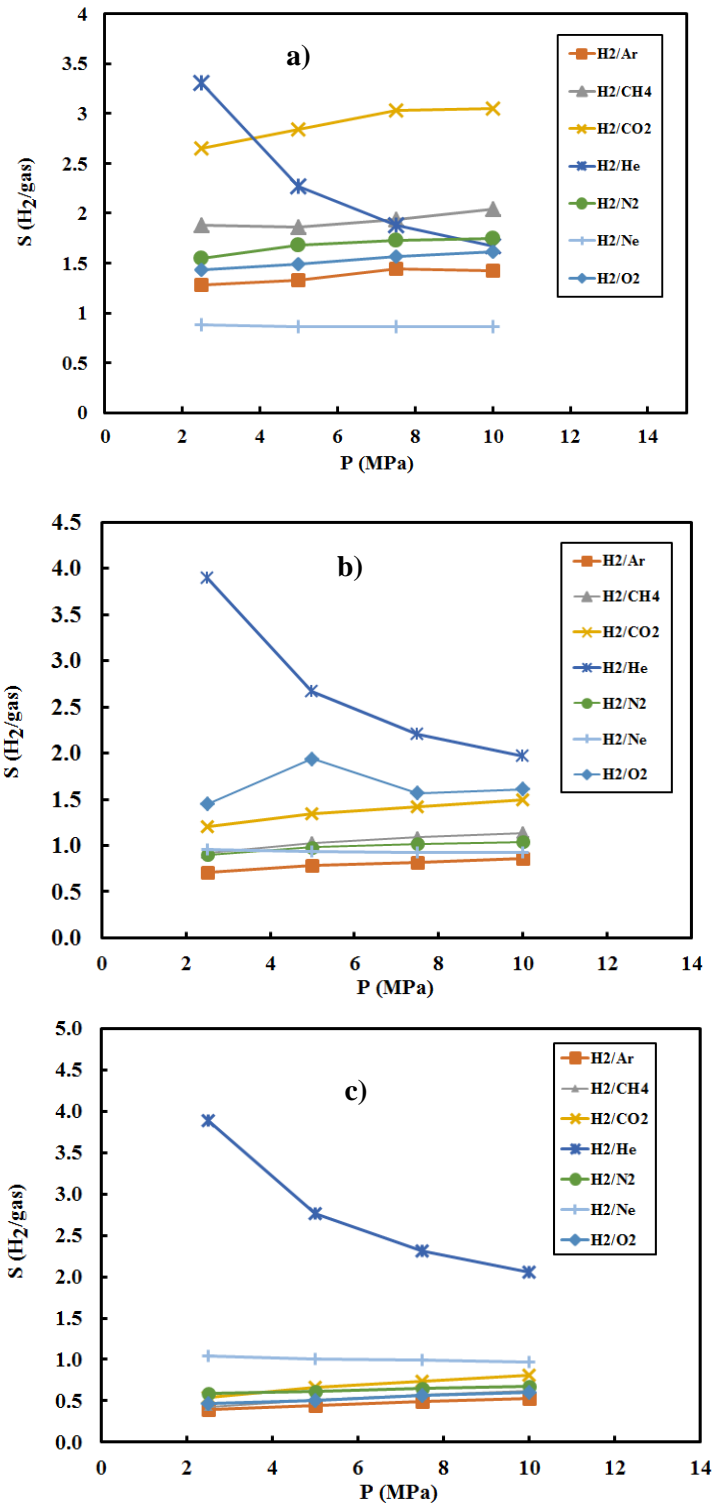
Figure 1. The selectivity of H_2/gas (a) in the (7,7) SWBNNT, (b) in the (15,15) SWBNNT, and (c) in the (29,29) SWBNNT at 146K and 1-10 MPa.

The adsorption selectivity of the binary mixtures of H_2/gas in the SWBNNTs at 0-1 MPa is provided in Figure 2. The calculated H_2/gas selectivity indicates that the H_2/He selectivity has the maximum values of 24.57, 29.07, and 19.81 in the (7,7), (15,15), and (29,29) SWBNNTs, respectively, and the values of the H_2/He selectivity decrease as pressure increases. Similarly, the slope of the H_2/Ne selectivity plot initially decreases and, then, reaches a plateau phase. The order of the selectivity values of other gases in the (7,7) and (15,15) SWBNNTs is as follows: H_2/CO_2> H_2/CH_4> H_2/N_2> H_2/O_2> H_2/Ar. Furthermore, these values of gas selectivity are lower than unity at low pressure, which is undesirable. However, the selectivity value slowly boosts as pressure increases. With increasing the tube diameter of the (29,29) SWBNNT, no significant difference is found between the values of the CO_2, CH_4, N_2, O_2, and Ar selectivity. These selectivity values are lower than unity, even at high pressure. Therefore, it can be declared that the best separation takes place in the tubes with smaller diameters at higher pressure.
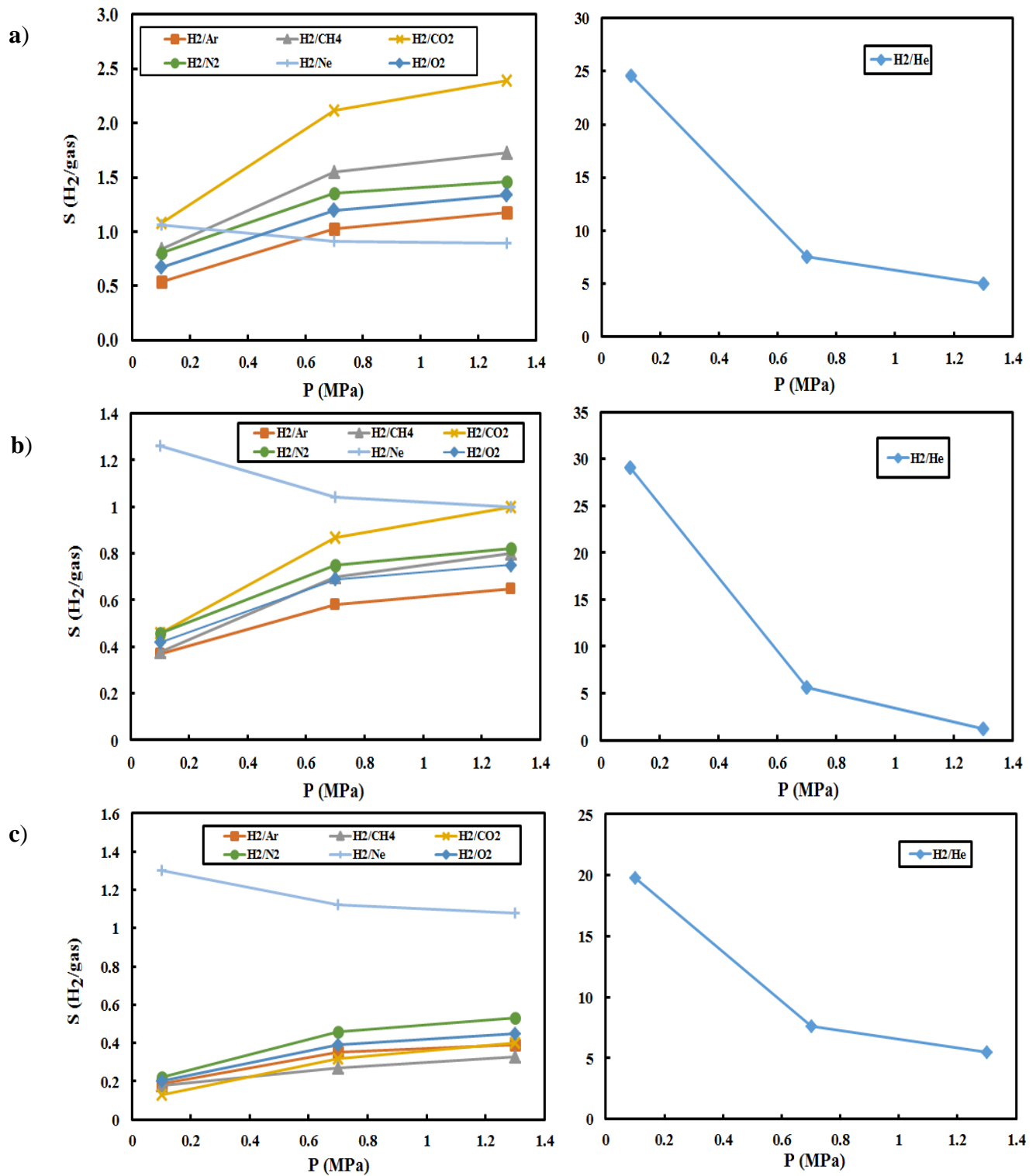
Figure 2. The selectivity of H_2/gas (a) within the (7,7) SWBNNT, (b) within the (15,15)

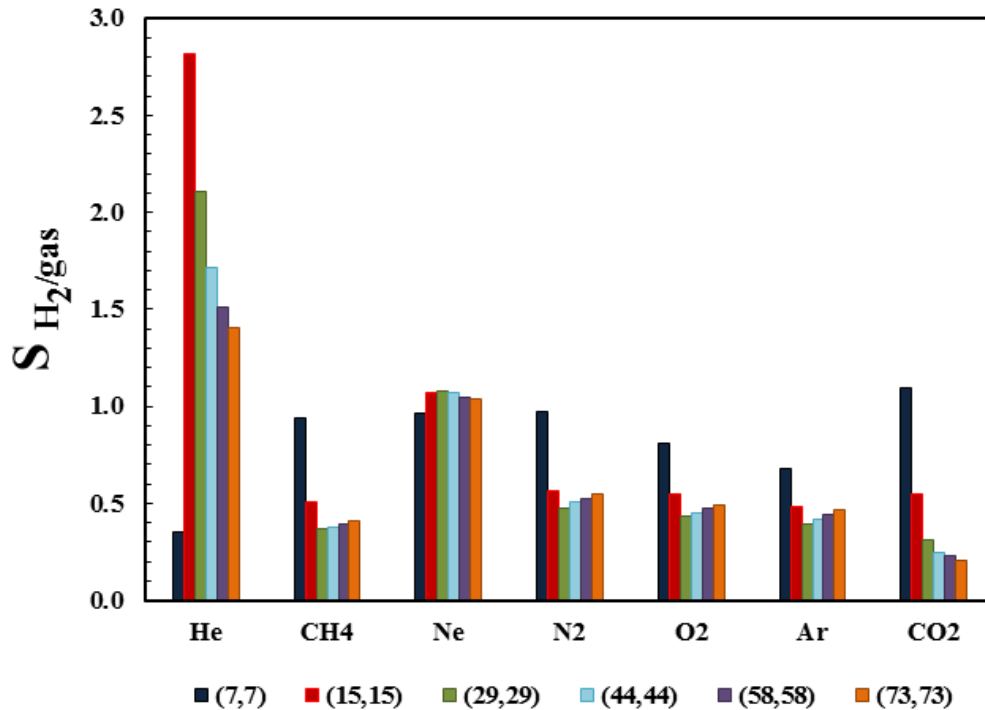SWBNNT, and (c) within the (29,29) SWBNNT at 146K and 0-1.5 MPa.

Figure 3. The comparison of the H_2/gas selectivity at 298K and 10MPa.

The values of the H_2/gas selectivity within the SWBNNTs at 298K and 10MPa are compared and the findings are shown in Figure 3. As indicated in Figure 3, H_2/He in the (15,15) SWBNNT and H_2/CO_2 in the (7,7) SWBNNT have the maximum and minimum values of the H_2/gas selectivity, respectively. The data also show that regardless of the selectivity value of H_2/He and H_2/Ne, the (7,7) SWBNNT has the maximum values of selectivity in the studied SWBNNTs.

On the whole, the results obtained from the H_2/gas separation within the SWBNNTs suggest that the best selectivity is achieved using He within small diameter tubes at high pressure.

3.2. H_2/gas selectivity in DWBNNTs

Hydrogen is separated from different gases inside the (11,11)@(15,15) and (7,7)@(22,22) double-walled BNNTs (DWBNNTs) at 298K and 10MPa via the simulation (see Figure 4).
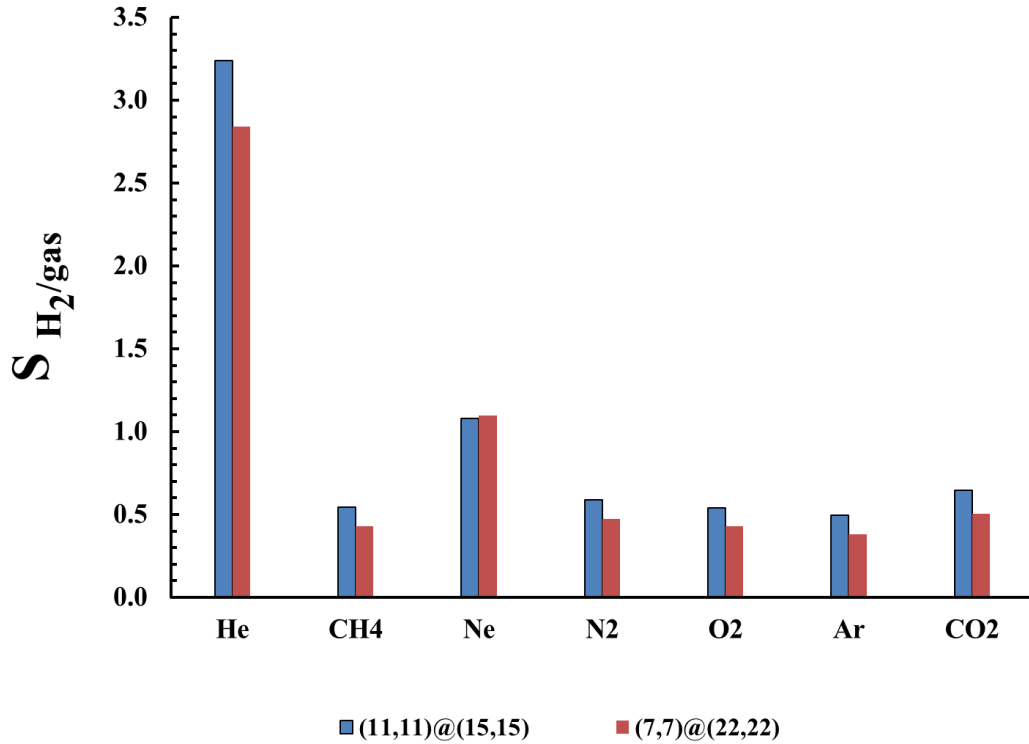
Figure 4. The H_2/gas selectivity of the DWBNNTs at 298 K and 10MPa.

As seen in Figure 4, the values of the H_2/gas selectivity indicate that the H_2/He selectivity has the maximum values in both DWBNNTs. Also, the H_2/He selectivity value in the (11,11)@(15,15) DWBNNT is more than that in the (7,7)@(22,22) DWBNNT. The binary mixture of H_2/Ar in the (7,7)@(22,22) DWBNNT has the minimum selectivity value.

3.3. H_2/gas selectivity in TWBNNTs

The separation of H_2 from the studied gases (i.e., Ar, CH_4, CO_2, He, N_2, Ne, and O_2) is investigated inside the (8,8)@(11,11)@(15,15) and (7,7)@(15,15)@(22,22) triple-walled BNNTs (TWBNNTs) at 298K and 10MPa (see Figure 5).
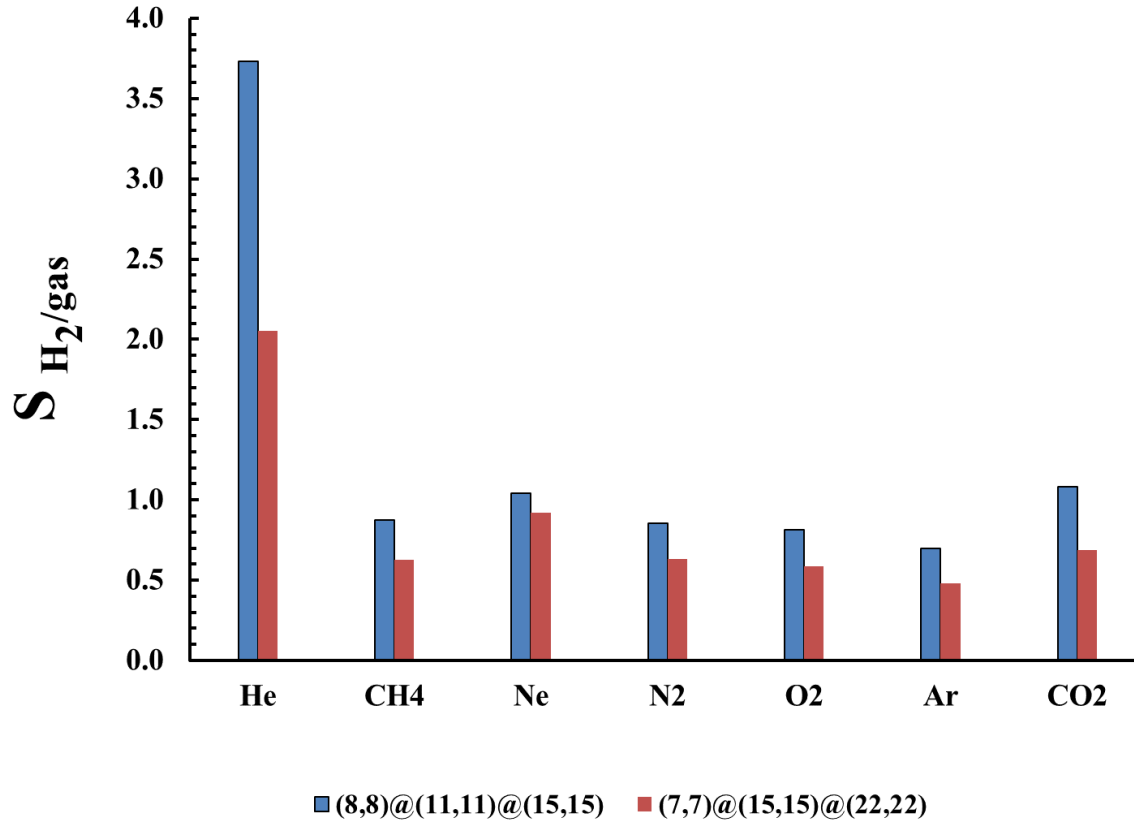
Figure 5. The H_2/gas selectivity inside the TWBNNTs at 298K and 10MPa.

As observed in Figure 5, H_2/He in the (8,8)@(11,11)@(15,15) TWBNNT and H_2/Ar in the (7,7)@(15,15)@(22,22) TWBNNT have the maximum and minimum values of selectivity, respectively.

3.4. The effect of temperature on selectivity

To study the impact of temperature on selectivity, the H_2/gas selectivity in the SWBNNTs is calculated at 293K, as depicted in Figure 6.
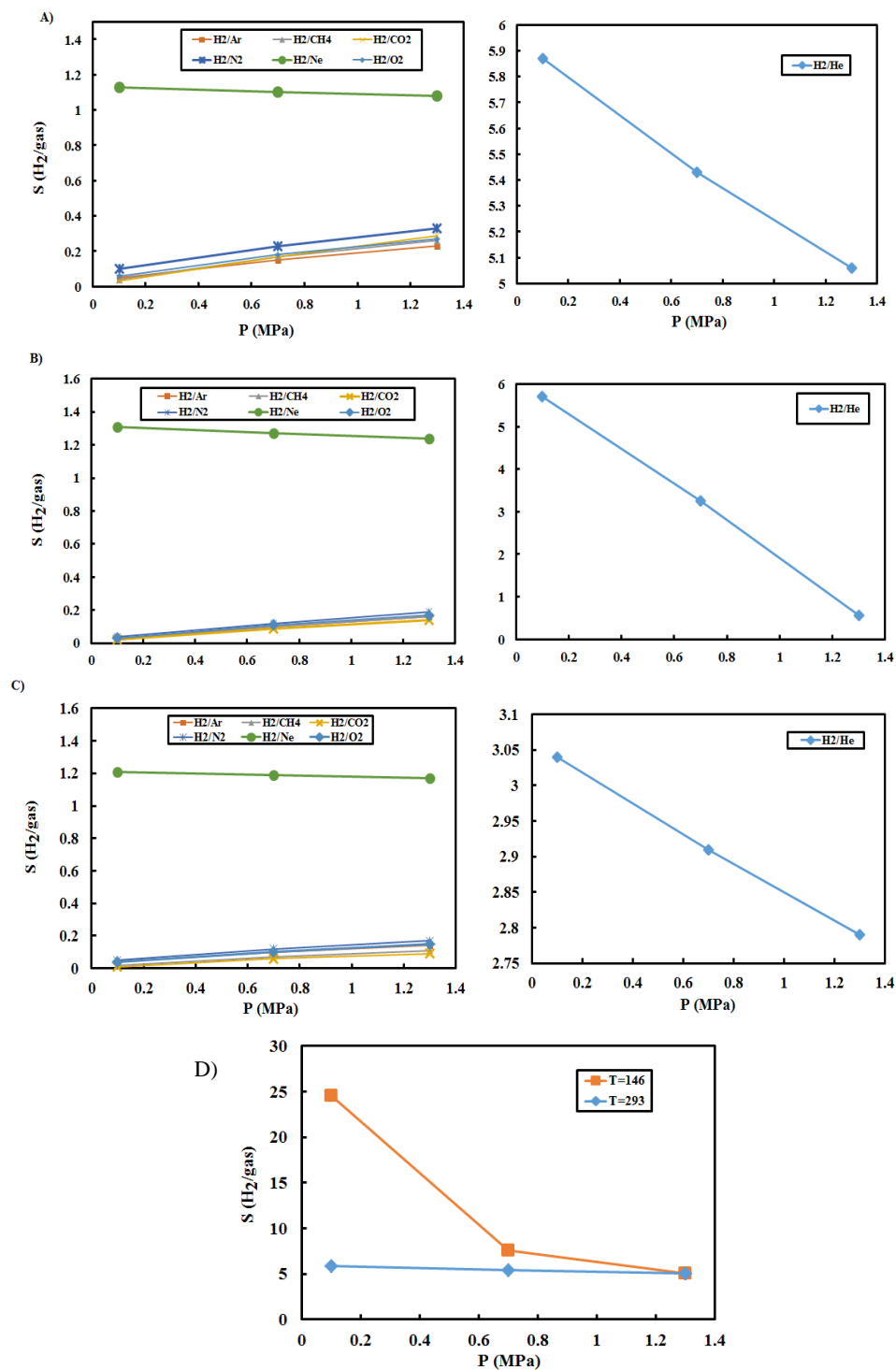
Figure 6. The H_2/gas selectivity (a) in the (7,7) SWBNNT, (b) in the (15,15) SWBNNTs, and (c) in the (29,29) SWBNNTs at 293K and at low pressure, and (d) in the (7,7) SWBNNT at 146K and 293K and at low pressure.

As illustrated in Figure 6, in the separation of hydrogen from the studied gases, the number of H_2 molecules as well as the selectivity values decreases as temperature increases.

In the next step of the simulation of the hydrogen separation from the gases, two other cases are considered. In both cases, the gases are simulated using the site-site model with atomic partial charges. However, just in one of the cases, the atoms of the (7,7) nanotube are charged. Figure 7 shows the separation of H_2/gas at 1atm. The simulation is also performed at 7 and 13atm and no significant change is found in the separation values at higher pressure.
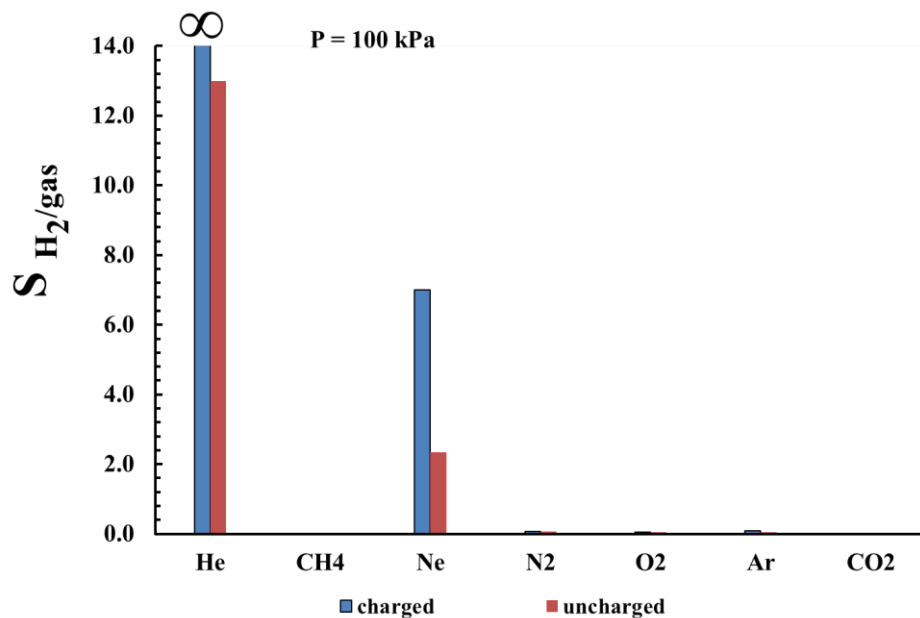

Figure 7. The role of the site-site model of the gases with and without atomic charges in the nanotubes

The obtained results clearly reveal that the hydrogen separation from He and the hydrogen separation from Ne have the best selectivity values. The results also show that there is no

significant difference in the results of the H_2 separation even when nanotube atomic charges are applied.

3.5. Comparison with other experimental and theoretical data

It should be noted that according to our knowledge there are not available experimental data for separation of hydrogen from binary mixtures within BNNTs. Therefore, for the last investigation, here we compare the results of the separations with those of the previous theoretical studies considered other nanotubes.

3.5.1 Comparison H_2/CH_4

Investigation of H_2/CH_4 separation on silicon nanotubes were studied by multiscale method [34]. They could find that the best selectivity of methane over hydrogen is about 4.25 (for H_2/CH_4 is 0.4) at slightly low than 10MPa, whereas Figure 5 shows the separation value for this binary mixture is about 8 (8 > 0.4) and takes place in (8,8)@(11,11)@(15,15) TWBNNT. However, according to our Figure 4, we can find that this separation value inside (11,11)@(15,15) DWBNNT is about 0.5. In another study experimentally found that the separation of H_2/CH_4 inside aligned carbon nanotube (CNT) was obtained about 2.58 [35] while within a kind of zeolite imidazolate frameworks; ZIF-8, it was about 9.8 [35] that is close to our data for TWBNNT. Therfore, a similar pattern of results was obtained, while our results suggest that multi-walled BNNTs are much more convenient than other nanotubes for separation of hydrogen over methane.

3.5.2 Comparison H_2/Ar, H_2/Ne

The best separation of H_2/Ar in our work is about 1.2 ($\approx$2MPa, 146K) inside (7,7) SWBNNT (Figure 1-a), while for a CNT was 4.14 (300K) [35]. So, it was included to verify that BNNTs may not be a suitable nano-structure for the separation of hydrogen over argon, however, more

research is necessary. In addition, the best separation of H_2/Ne in our work is about 1.3 ($\approx$0.1MPa, 146K) inside (29,29) SWBNNT (Figure 2-c), and with changing single-walled to triple-walled, this value remains constant. According to the author's investigations there is not any report here to compare results.

3.5.3 Comparison H_2/CO_2, H_2/N_2 and H_2/O_2

For H_2/N_2 and H_2/O_2, the separation values reported by CNTs is 3.48 and 3.82 respectively [35] and our results is 1.5 and 1.25 respectively ($\approx$1.3MPa, 146K within (7,7) SWBNNT (Figure 2-a)). Another report showed that the for H_2/N_2 and H_2/O_2, the Knudsen selectivities is 2.75 and 4 respectivley under 2 atm pressure gradient with the aligned CNT derived from ferrocene/camphor and temperature of 20-70°C [36]. By comparing the results of Ref. [35] and [36] with our obtained data, we can realize that to improve the gas separation performance, the aligned nanotubes including functional groups can work well.

Furthermore, the separation values for H_2/CO_2 were reported 4.89 (300K) [35] and 4 (20-70°C) in aligned CNTs [36]. Whereas we have obtained it around 3 in the (7,7) SWBNNT at 146K and 8MPa. However, selectivity should be independent of temperature, so selectivity changes at different temperatures. Thus, in order to have the best comparison, both thermodynamics and structural factors of nano-structures must be considered in the next investigations.

3.5.4 Comparison H_2/He

The last comparison is the separation of H_2/He. The separation value of H_2/He was reported about 3.2 at room temperature that was investigated by molecular dynamics using surface activated CNTs [37]. Surprisingly, we have focused on single and triple walled BNNTs and have obtained the separation value for this mixture about 3.7 (triple and double walled at 298K and 10MPa) and about 30 ($\approx$0.2MPa and 146K) within the (15,15) SWBNNT. Perhaps, this yields

increasingly good results on separation of hydrogen over helium. At this stage of understanding, we believe that it needs more studies to find the mechanism of adsorption of hydrogen and helium together in nanotubes.

It is important to note, that the present evidence relies on BNNTs are proper for separation of hydrogen over methane and helium, in addition, several questions remain unanswered in this regard. By comparing the results from the next studies, we hope to determine the best aspect of view about the separation-based adsorption of binary mixtures gases within BNNTs.

4. Conclusion

This study is designed to investigate the separation of the binary mixtures of hydrogen and biogas, such as CO_2, CH_4, and O_2, as well as that of the binary mixtures of hydrogen and noble gases via adsorption on single-walled Boron Nitride Nanotubes (SWBNNTs) [for example, the (7,7), (15,15) and (29,29) SWBNNTs] and multi-walled Boron Nitride Nanotubes (MWBNNTs) [for example, the (15,15)@(11,11) and (22,22)@(7,7) DWBNNTs and the (15,15)@(11,11)@(8,8) and (22,22)@ (15,15)@((7,7) TWBNNTs] using the GCMC molecular simulations. The results show that the maximum value of the H_2/He selectivity is 30 in the (15,15) SWBNNT. It is also found that as pressure and temperature increase, the H_2/He selectivity in the studied BNNTs decreases. Ultimately, the findings indicate charging the atoms of nanotubes and using the site-site models for the gases cannot exert a significant influence on the H_2 separation.

References

[1] Z.Zhang, W.Guo, Y.Dai, Stability and electronic properties of small boron nitride nanotubes. J. Appl. Phys. 105, 084312 (2009).

[2] A.Rubio, J.L.Corkill, M.L.Cohen, Theory of graphitic boron nitride nanotubes. Phys. Rev. B, 49, 5081 (1994).

[3] N.G.Chopra, R.J.Luyken, K.Cherrey, V.H.Crespi, M.L.Cohen, S.G.Louie, A.Zettl, Boron nitride nanotubes. Science, 269, 966-967 (1995).

[4] C.Lee, S.Bhandari, B.Tiwari, N.Yapici, D.Zhang, Y.Yap, Boron nitride nanotubes: recent advances in their synthesis, functionalization, and applications. Molecules, 21, 922 (2016).

[5] T.Li, Z.Tang, Z.Huang, J.Yu, A comparison between the mechanical and thermal properties of single-walled carbon nanotubes and boron nitride nanotubes. Physica E: Low-dimensional Systems and Nanostructures, 85, 137-142 (2017).

[6] S.Abbas, A.Abbas, Y.Huang, J.Lin, Z.Liu, Y.Fang, C.Tang, Synthesis of boron nitride nanotubes using an oxygen and carbon dual-free precursor. RSC Adv. 8, 3989-3995 (2018).

[7] Ö.Şen,; Z.Çobandede, M.Emanet, Ö.F.Bayrak, M.Çulha, Boron nitride nanotubes for gene silencing. BBA-Gen. Subjects, 1861, 2391-2397 (2017).

[8] M.L.Cohen, A.Zettl, The physics of boron nitride nanotubes. Phys. Today, 63, 34-38 (2010).

[9] A.L.Tiano, L.Gibbons, M.Tsui, S.I.Applin, R.Silva, C.Park, C.C.Fay, Thermodynamic approach to boron nitride nanotube solubility and dispersion. Nanoscale, 8, 4348-4359 (2016).

[10] J.Wang, C.H.Lee, Y.Bando, D.Golberg, Y.K.Yap, Multiwalled boron nitride nanotubes: growth, properties, and applications. In BCN Nanotubes and Related Nanostructures (pp. 23-44). Springer, New York, NY. (2009).

[11] C.Tang, Y.Bando, T.Sato, K.Kurashima, A novel precursor for synthesis of pure boron nitride nanotubes. Chem. Commun. 12, 1290-1291 (2002).

[12] M.Rousseas, A.P.Goldstein, W.Mickelson, M.A.Worsley, L.Woo, A.Zettl, Synthesis of highly crystalline sp^2-bonded boron nitride aerogels. ACS nano, 7, 8540-8546 (2013).

[13] H.Du, J.Li, J.Zhang, G.Su, X.Li, Y.Zhao, Separation of hydrogen and nitrogen gases with porous graphene membrane. J. Phys. Chem. C, 115, 23261-23266 (2011).

[14] Y.Chen, J.Jiang, A bio-metal–organic framework for highly selective CO_2 capture: A molecular simulation study. ChemSusChem, 3, 982-988 (2010).

[15] G.Mpourmpakis, G.E.Froudakis, Why boron nitride nanotubes are preferable to carbon nanotubes for hydrogen storage?: An ab initio theoretical study. Catal. Today, 120, 341 (2007).

[16] M.U.Niemann, S.S.Srinivasan, A.R.Phani, A.Kumar, D.Y.Goswami, E.K.Stefanakos, Nanomaterials for hydrogen storage applications: a review. J. Nanomater. (2008) DOI: 10.1155/2008/950967.

[17] D.Cao, J.Wu, Modeling the selectivity of activated carbons for efficient separation of hydrogen and carbon dioxide. Carbon, 43, 1364-1370 (2005).

[18] N.O.Chisholm, G.C.Anderson, J.F.McNally, H.H.Funke, R.D.Noble, J.L.Falconer, Increasing H_2/N_2 separation selectivity in CHA zeolite membranes by adding a third gas. J.Membr. Sci. 496, 118-124 (2015).

[19] R.Antunes, O.Borisevich, D.Demange, Numerical analysis of H_2/He gas separation experiments performed with a MFI-type tubular zeolite membrane. Chem. Eng. Res. Des. 109, 327-334 (2016).

[20] K.Ghasemzadeh, S.M.S.Tilebon, A.Basile, Silica Membranes Application for Hydrogen Separation. In Current Trends and Future Developments on (Bio-) Membranes (pp. 243-264). Elsevier. 2017.

[21] C.Gu, G.H.Gao, Y.X.Yu, T.Nitta, Simulation for separation of hydrogen and carbon monoxide by adsorption on single-walled carbon nanotubes. Fluid Phase Equilibria, 194, 297-307 (2002).

[22] H.Chen, D.S.Sholl, Predictions of selectivity and flux for CH4/H2 separations using single walled carbon nanotubes as membranes. J. Membr. Sci. 269, 152-160 (2006).

[23] B.Zhou, W.Li, J.Zhang, Theoretical simulation of CH_4 separation from H_2 in CAU-17 materials. J. Phys. Chem. C, 121, 20197-20204 (2017).

[24] F.A.Kloutse, A.Hourri, S.Natarajan, P.Benard, R.Chahine, Hydrogen separation by adsorption: Experiments and modelling of H_2-N_2-CO_2 and H_2-CH_4-CO_2 mixtures adsorption on CuBTC and MOF-5. Micro. Meso. Mate. 271, 175-185 (2018).

[25] L.Bastin, P.S.Bárcia, E.J.Hurtado, J.A.Silva, A.E.Rodrigues, B.A.Chen, Microporous metal−organic framework for separation of CO_2/N_2 and CO_2/CH_4 by fixed-bed adsorption. J. Phys. Chem. C, 112, 1575-1581 (2008).

[26] M.Shadman, Z.Ahadi, Argon and neon storages in single-walled boron nitride nanotubes: a grand canonical Monte-Carlo study. Fullerenes, Nanotubes and Carbon Nanostructures, 19, 700-712 (2011).

[27] M.A.Bagherinia, M.Shadman, Investigations of CO_2, CH_4 and N_2 physisorption in single-walled silicon carbon nanotubes using GCMC simulation. Int. Nano Lett. 4, 95 (2014).

[28] S.Taheri, M.Shadman, A.Soltanabadi, Z.Ahadi, Grand canonical Monte Carlo simulation of hydrogen physisorption in Li-and K-doped single-walled silicon carbide nanotube. Int. Nano Lett. 4, 81-90 (2014).

[29] M.Shadman, S.Yeganegi, M.R.Galugahi, Hydrogen physisorption and selectivity in single-walled silicon carbon nanotubes: a grand canonical Monte-Carlo study. J.Iran. Chem. Soc. 13, 207-220 (2016).

[30] A.Gupta, S.Chempath, M.J.Sanborn, L.A.Clark, R.Q.Snurr, Object-oriented programming paradigms for molecular modeling. Mol. Simul. 29, 29-46 (2003).

[31] Z.Ahadi, M.Shadman, S.Yeganegi, F.Asgari, Hydrogen adsorption capacities of multi-walled boron nitride nanotubes and nanotube arrays: a grand canonical Monte Carlo study, Journal of molecular modeling, 18, 2981-2991 (2012).

[32] M.Shadman, S.Yeganegi, F.Ziaie, Ab initio interaction potential of methane and nitrogen, Chemical Physics Letters, 467, 237-242 (2009).

[32] A.Shahsavani, Z.Ahadi, V.Sokhanvaran, M.Taghizadeh, M.Hadei, M.Shadman Lakmehsari, Dynamics and Separation-based Adsorption of Binary Mixtures of CH_4, CO_2 and H_2S on MIL-47: GCMC and MD Studies, J. Nanoanalysis, 6,48-59 (2019).

[33] C.Y.Won, and N.R.Aluru, Structure and dynamics of water confined in a boron nitride nanotube, J. Phys. Chem. C, 112, 1812-1818 (2008).

[34] S. Balilehvand, S.M. Hashemianzadeh, S.S. Razavi and H. Karimi, Investigation of hydrogen and methane adsorption/separation on silicon nanotubes: a hierarchical multiscale method from quantum mechanics to molecular simulation, Adsorption, 18, 13–22 (2012).

[35] L. Ge, A. Du, M. Hou, V. Rudolpha and Z. Zhu, Enhanced hydrogen separation by vertically-aligned carbon nanotube membranes with zeolite imidazolate frameworks as a selective layer, RSC Adv., 2, 11793–11800 (2012).

[36] L. Ge, L. Wang, A.Du, M. Hou, V. Rudolpha and Z. Zhu, Vertically-aligned carbon nanotube membranes for hydrogen separation, RSC Adv., 2, 5329–5336 (2012).

[37] Z. Insepov and R.J. Miller, Activation of Nanoflows for Fuel Cells, J. Nanotech. Eng. Medicine, 3, 025201 (2012).